JOURNAL OF CATALYSIS 100, 95–102 (1986)

Structural, Surface, and Catalytic Properties of Bismuth Molybdovanadates Containing Foreign Atoms[1]

II. Propene Oxidation on Iron-Containing Bismuth Molybdovanadate Catalysts

SERGIO DE ROSSI, MARIANO LO JACONO, PIERO PORTA,[2] MARIO VALIGI, DELIA GAZZOLI, GIULIANO MINELLI, AND ANNA ANICHINI

Centro di Studio del Consiglio Nazionale delle Ricerche (CNR) su "Struttura e Attività Catalitica di Sistemi di Ossidi" (SACSO), % Dipartimento di Chimica, Università "La Sapienza," 00185 Roma, Italy

Received February 25, 1985

The selective oxidation of propene to acrolein has been studied on iron-containing bismuth molybdovanadates with the scheelite structure and general formula $Bi_{1-x/3}\square_{x/3-y}Me_y(V_{1-x}Mo_{x-y}Fe_y)O_4$, where *Me* = Fe or Bi, □ = cation vacancy, with $x = 0.45$ and 0.60 and $0 \leq y \leq x/3$, using the pulse technique in the temperature range 573–673 K. Total conversion, rate constant, and selectivity were found to depend on catalyst composition, in particular cation vacancy concentration, content, and coordination symmetry of the iron ions. The results, discussed in terms of compositional parameter *y* and surface geometry of Bi–O and Mo–O species, confirm the importance of the cation vacancies in the selective oxidation process and suggest a role of the eight-coordinated cations in the allyl formation.

INTRODUCTION

The selective (ammo)oxidation of propene over mixed oxide catalyst systems is a process of great industrial importance and academic interest. For this reason it has been extensively studied and discussed in several reviews (*1–4*).

However, while efforts in catalyst development and in providing a kinetic model have been quite successful, there is much uncertainty concerning the structure of intermediates and the exact role of the individual metallic component of the catalyst in the various reaction steps (*1, 2, 5, 6*).

A comparison between the more important proposed mechanisms for the selective oxidation of propene on molybdenum-based catalysts shows that authors agree upon the stages of the process, namely initial chemisorption of the olefin, α-hydrogen abstraction and allyl intermediate formation, and so on, but disagree upon the metal centers operating as the active sites in each stage. As an example, some authors (*7, 8*) attribute initial chemisorption and first hydrogen abstraction to anion vacancies associated with molybdenum, while according to the mechanism proposed by Haber, the same reaction steps occur on bismuth as a result of its high dehydrogenating ability (*9, 10*).

In the case of catalysts possessing the scheelite structure, other authors (*2, 11*) attribute both these reaction steps to $(MoO_4)^{2-}$ groups, emphasizing the important role of A cation vacancies which, accepting and stabilizing the α-hydrogen abstracted from olefins during the allyl formation, are considered to be responsible for the rate-controlling step.

However, Grasselli *et al.* (*1, 5*), by mechanistic studies, have concluded that initial chemisorption occurs on coordinatively unsaturated molybdenum centers, while allylic abstraction takes place on oxygens bonded to bismuth. Brazdil *et al.* (*12*), reex-

[1] This work has been supported by a financial contribution from the "Progetto Finalizzato (CNR) on Chimica Fine e Secondaria."

[2] To whom correspondence should be addressed.

0021-9517/86 $3.00

amining the role of bismuth and of the A cation vacancies in doped scheelite–molybdate catalyst systems for the selective ammoxidation of propene, confirm the previous general mechanistic scheme (*1, 5*), and conclude that cation vacancies in a scheelite structure are not directly involved in this rate-determining hydrogen abstraction step.

In order to clarify some of the doubts and uncertainties which have arisen in the literature, we have undertaken an investigation on iron-promoted bismuth molybdovanadates with the aim of defining the structural properties (*13, 14*) and of clarifying the relationship between these and the catalytic behavior. These catalysts with scheelite structure and of general formula $Bi_{1-x/3}\square_{x/3-y}Me_y(V_{1-x}Mo_{x-y}Fe_y)O_4$, ($Me$ = Fe or Bi, $0 \leq y \leq x/3$) offer a wide variety of chemistry and are ideal for studying the relationship between structure and catalytic properties.

The present paper reports catalytic results on the oxidation of propene to acrolein, as studied by a microcatalytic pulse technique.

EXPERIMENTAL

Catalysts. All specimens were prepared by a coprecipitation method and a final calcination at 873 K in air. Details of preparative procedures adopted and of catalyst characterization have been described earlier (*13, 14*).

With reference to the general formula, the catalytic results refer to four series of specimens obtained by taking samples with fixed x value (0.45 and 0.60) and y in the range from 0 to $x/3$. Both cases for which Me = Fe and Me = Bi were considered.

Apparatus and procedure. The oxidation of propene was studied using a microcatalytic pulse reactor at temperatures of 573, 623, and 673 K. The system included a conventional Pyrex reactor, vertically positioned in an electrical furnace and containing 1 g of powdered catalyst, a glass vacuum section with a dosing device of 0.5 cm^3 and a U-tube manometer, and an ATC/F C.Erba gas chromatograph connected to a 3370A Hewlett–Packard integrator. At time intervals of 45 min, pulses (5–8 for each run) of reactant mixture (3.5 μmol of O_2 and 3.5 μmol of C_3H_6) were carried over the catalyst by a helium gas stream of 20 $cm^3\ min^{-1}$ flow rate.

The analysis of the reaction products, performed with an estimated accuracy within ± 0.05 μmol, was carried out in two steps. In the first step O_2 and CO were separated in a 1-m steel column of 4 mm i.d., filled with a 5A molecular sieve and thermostated at 353 K, while the other products were condensed in a trap at 77 K located at the exit of the reactor. In the second step the trap was rapidly warmed up and the analysis of CO_2, C_3H_6, H_2O, and C_3H_4O was performed in a 4-m steel column of 4 mm i.d., filled with Porapak R and thermostated at 419 K.

The propene conversion and acrolein molar selectivity were calculated according to

$$\% \text{ Conversion} = \frac{C_3H_{6\,(in)} - C_3H_{6\,(out)}}{C_3H_{6\,(in)}} \times 100$$

$$\% \text{ Molar Selectivity} = \frac{C_3H_4O}{C_3H_{6\,(in)} - C_3H_{6\,(out)}} \times 100.$$

Catalyst pretreatment. Before each series of experiments, a standard pretreatment in oxygen flow was carried out at 723 K overnight, followed by a conditioning with He flow at the same temperature for 30 min. The catalysts could be repeatedly used and a very good reproducibility was found.

RESULTS

The catalytic behavior of $Bi_{1-x/3}\square_{x/3-y}Me_y(V_{1-x}Mo_{x-y}Fe_y)O_4$ solid solutions in the pulse oxidation of propene generally fell to fairly constant values after the first couple of pulses; an example is shown in Fig. 1.

Data corresponding to these lined-out

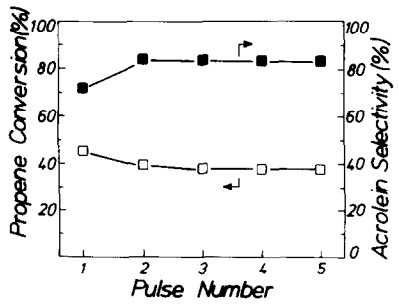

FIG. 1. Catalytic activity and selectivity at 623 K for propene oxidation for $Bi_{1-x/3}\square_{x/3-y}Me_y(V_{1-x}Mo_{x-y}Fe_y)O_4$ system (with $x = 0.60$, $y = 0.10$ and Me = Bi) as a function of the pulse number.

values for propene conversion and selectivity to acrolein at 573, 623, and 673 K are summarized in Figs. 2 and 3, for $x = 0.45$ and 0.60, respectively, as a function of the structural composition parameter y.

From inspection of Figs. 2 and 3 and referring to the general formula of the solid solutions, it appears that a different activity and selectivity trend occurs for catalyst series with same x (0.45 or 0.60) and different

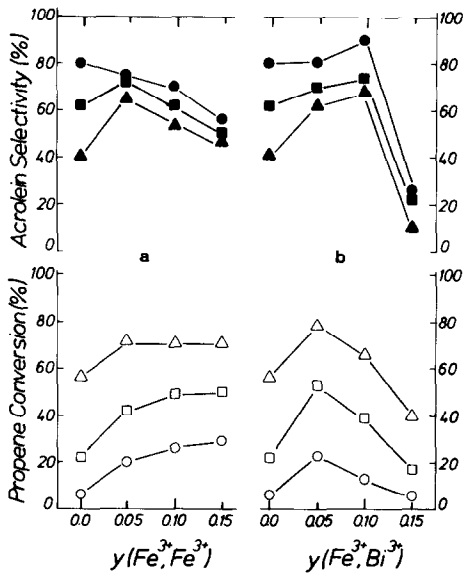

FIG. 2. Catalytic activity and selectivity for propene oxidation for $Bi_{1-x/3}\square_{x/3-y}Me_y(V_{1-x}Mo_{x-y}Fe_y)O_4$ system (with $x = 0.45$ and Me = Fe or Bi) as a function of y; (○,●) 573 K; (□,■) 623 K; (△,▲) 673 K.

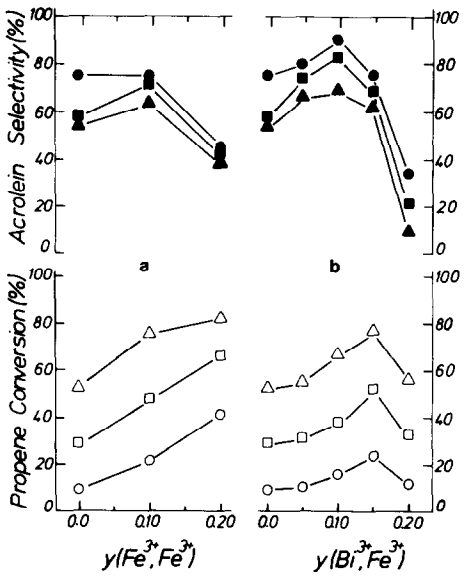

FIG. 3. Catalytic activity and selectivity for propene oxidation for $Bi_{1-x/3}\square_{x/3-y}Me_y(V_{1-x}Mo_{x-y}Fe_y)O_4$ system (with $x = 0.60$ and Me = Fe or Bi) as a function of y; (○,●) 573 K; (□,■) 623 K; (△,▲) 673 K.

Me (Fe and Bi). On the other hand, a similar activity and selectivity tendency exists for catalyst series with different x (0.45 and 0.60) and the same Me (Fe or Bi).

At a given temperature the propene conversion per gram of catalyst generally increases with y for both ($x = 0.45$ and 0.60) specimens, with Me = Fe, while for specimens with Me = Bi it achieves a maximum at an intermediate value of y and then decreases.

The selectivity to acrolein at first generally increases with y, then decreases for y tending to the limit values of 0.15 (Fig. 2) or 0.20 (Fig. 3). This behavior is particularly marked for the series with Me = Bi.

It should be noted that when $y = 0.15$ and $y = 0.20$ for the series $x = 0.45$ and $x = 0.60$, respectively, there are no cation vacancies in the structure.

Thus the complete filling of the eight-coordinated cation vacancies produces a drop in selectivity, while for the catalytic activity the decrease is evident only for the catalyst series with Me = Bi.

However, to compare correctly with catalytic results and structural parameters, it is vital to calculate the kinetic rate constant per unit of surface area of the catalyst (k_{sp}). This can be done on the basis of a first-order kinetic equation with respect to propene (*2, 12, 15, 16*) and by taking into account that, under conditions of low reactant partial pressure, the kinetic rate constant and the fractional conversion X of a pulse of reactant passed through a catalyst column are related by the equation (*17*)

$$\ln[1/(1 - X)] = (RTW/F)kK \qquad (1)$$

where F is the flow rate of the carrier gas in the reactor, k the kinetic constant for a first-order reaction, K the adsorption equilibrium constant of reactant, and W the catalyst weight.

However, the use of Eq. (1) for propene oxidation (which is formally bimolecular) implies the assumption of zero-order kinetics with respect to oxygen, and in fact this is commonly found for systems such as those investigated in this work where lattice oxygen is the major or sole oxidant (*2, 12, 15, 16*).

A constant term which takes into account the zero-order dependence on oxygen should in principle appear in Eq. (1) (as well as in the following Eq. (2)), but it is omitted here since it will not affect the comparison of the activity among the different catalysts.

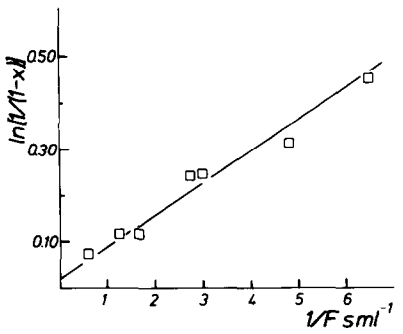

FIG. 4. Test of first-order rate law for propene oxidation at 623 K on 1 g of $Bi_{1-x/3}\square_{x/3-y}Me_y(V_{1-x}Mo_{x-y}Fe_y)O_4$ sample (with $x = 0.45$ and $y = 0.00$).

Equation (1) is analogous to that which holds in a conventional steady-state flow reactor

$$\ln[1/(1 - X)] = (V/F)k \qquad (2)$$

where V is the volume of the catalyst.

As an example, Fig. 4 shows that, over the studied range, Eqs. (1) and (2) are obeyed and therefore the reaction is first-order. The apparent activation energy E_a may then be obtained at a constant flow rate of the carrier gas from the slope of a plot of $\ln\{\ln[1/(1 - X)]\}$ vs $1/T$.

Since one of the aims of the present work is the comparison of the specific activity among the various catalysts and its correlation with the compositional parameters, we used for the calculation of the kinetic constants the simpler Eq. (2). Table 1 summarizes the values of surface area, kinetic constant k_{sp} and apparent activation energy E_a for the specimens studied.

It is immediately evident that the values of the specific constants of the catalysts with Me = Bi and no vacancies are comparatively very low. This is not the case, except at the highest reaction temperature, for the catalysts with Me = Fe and no vacancies, where the comparative decrease of k_{sp} is nevertheless less pronounced. Hence, the presence of cation vacancies in our scheelite structures is a prerequisite for the propene selective oxidation at least in the case where eight-coordinated iron is absent.

Our results also show that the presence of iron, while having small effect on the specific rate constant, generally improves the selectivity to acrolein (see Figs. 2 and 3) and does decrease the apparent activation energy of the reaction in comparison with the bismuth molybdovanadate with the same value of x (0.45 or 0.60) (see Table 1).

DISCUSSION

The results of our study show how the catalytic activity and selectivity correlate with the variation of the structural compositional parameter, y, along each series of

TABLE 1

Kinetic Parameters for Oxidation of Propene over $Bi_{1-x/3}\square_{x/3-y}Me_y(V_{1-x}Mo_{x-y}Fe_y)O_4$ Catalysts

Compositional parameters of catalysts				Surface area ($m^2\ g^{-1}$)	Rate constant k_{sp} ($s^{-1}\ m^{-2}$)			E_a (kJ mol^{-1})
x	y	$\square_{x/3-y}$	Me		573 K	623 K	673 K	
0.45	0.00	0.15		0.7	0.05	0.20	0.65	84
0.45	0.05	0.10	Bi	1.3	0.11	0.32	0.65	54
0.45	0.10	0.05	Bi	0.8	0.10	0.34	0.75	63
0.45	0.15	0.00	Bi	3.8	0.01	0.03	0.08	67
0.45	0.05	0.10	Fe	1.3	0.10	0.23	0.53	54
0.45	0.10	0.05	Fe	1.5	0.11	0.25	0.45	46
0.45	0.15	0.00	Fe	2.0	0.10	0.20	0.33	42
0.60	0.00	0.20		0.8	0.07	0.24	0.51	67
0.60	0.05	0.15	Bi	1.0	0.07	0.21	0.44	63
0.60	0.10	0.10	Bi	1.2	0.08	0.22	0.51	59
0.60	0.15	0.05	Bi	1.7	0.09	0.24	0.48	54
0.60	0.20	0.00	Bi	5.6	0.01	0.04	0.08	59
0.60	0.10	0.10	Fe	1.4	0.09	0.26	0.55	54
0.60	0.20	0.00	Fe	3.5	0.08	0.17	0.27	38

catalysts with constant x value ($x = 0.45$ or $x = 0.60$).

When the cation vacancy level, associated with the y parameter by the relation $x/3 - y$, is decreased with a constant or increasing bismuth level (series with Me = Fe and Me = Bi, respectively), both catalytic activity (Table 1) and selectivity (Figs. 2 and 3) significantly decrease.

However, a significant difference in the catalytic behavior exists between the solid solution systems with Me = Fe and that with Me = Bi. In fact for the latter one, the catalytic activity and selectivity dramatically drop with the complete filling of the cation vacancies, namely for $y = x/3$, despite the fact that the bismuth concentration is actually increased.

If the general mechanistic scheme for bismuth and molybdenum oxide based catalysts requires the formation of the allylic intermediate by the abstraction of an α-hydrogen from propene (*3, 5, 18–20*), then, regardless of whether the chemisorption of olefin takes place on Bi (*9, 10*) or on Mo (*1, 2, 7, 8*) sites, our results support the conclusion of Sleight (*2*) that cation vacancies associated with bismuth in a scheelite structure are involved in the rate-determining hydrogen abstraction step, probably by favoring and stabilizing the formation of the hydroxyl group at the surface of the catalyst.

However, this does not mean that bismuth is not significantly and directly involved in the important step of α-hydrogen abstraction. In fact, on the one hand the high dehydrogenation ability of bismuth cannot be ignored (*5, 10, 12*) and on the other hand the presence of cation vacancies, causing a variation in the bulk trigonal coordination of oxygen (*14*), type *a* of Fig. 6, can influence the formation of the hydroxyl group on both Bi and Mo.

Indeed the unsaturation of the oxygen ions, enhancing their basic character, can favor the abstraction of the allyl hydrogen, irrespectively of where olefin adsorption takes place. Moreover, the effects of cation vacancies on oxygen coordination and therefore on catalytic behavior will appear amplified at the surface, since defects will tend to concentrate at the surface (*11*).

A description of the changes which occur

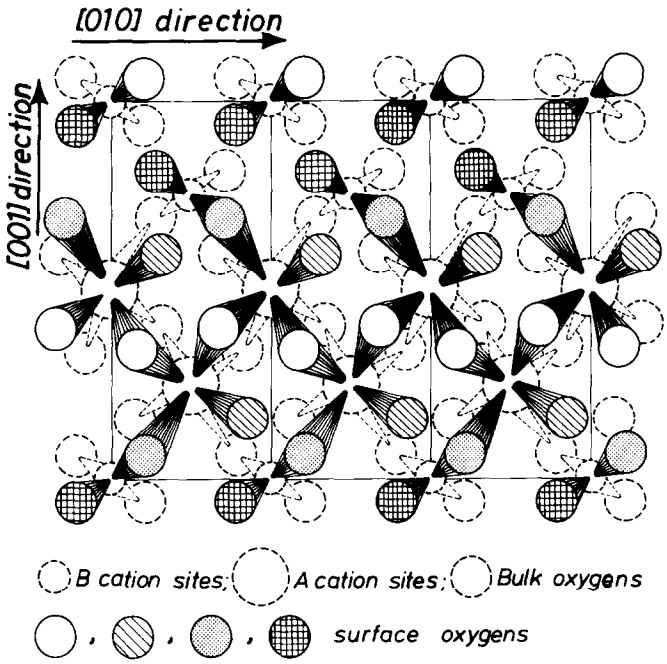

FIG. 5. Schematic representation of the (100) plane of scheelite. The tetrahedral B cation sites can be vanadium, molybdenum, or iron; the eight-coordinated A cation sites can be bismuth, iron, or vacancy; key to symbols of surface oxygen in Fig. 6.

on creation of one surface Bi vacancy requires a knowledge of both the initial and final state of the system. For the present purposes we wish to examine in some detail, as an example, the (100) planes and extend the conclusion to other planes such as (101) or (111).

The atomic occupancy on the (100) plane is schematically shown in Fig. 5, where three unit cells are represented. It is evident that between two oxygen layers both eight-coordinated and tetrahedral cationic sites are present. The cation arrangement, perpendicular to the [001] direction and moving along the [010] direction in Fig. 5, is such that two rows of tetrahedral cations and two rows of eight-coordinated cations are alternatively encountered.

It can be reasonably assumed that the crystal terminates with an anion layer of both O^{2-} and $(OH)^-$ groups. If for simplicity the OH groups are neglected for a moment, different types of capping oxygen anions on the (100) surface layer are present. The coordination types of these oxygen anions are schematically illustrated in Fig. 6: type *b* represents an oxygen bonded to two eight-coordinated A cation sites and having one vacant tetrahedral B cation site; types *c* and *e* depict an oxygen anion bonded only to one A cation site and to one B cation site, respectively; type *d* depicts an oxygen bonded to one A cation site and to one B cation site, and having one missing coordination (A cation site). The four types of uncoordinated surface oxygen anions, *b*, *c*, *d*, and *e*, exist in the ratio 2 : 2 : 2 : 2 for each unit cell and constitute groups of atoms and vacancies periodically repeated, namely

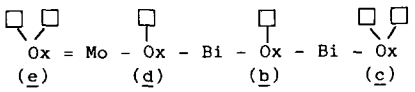

Each A cation site has four bulk oxygen anions of type *a* and four surface oxygens:

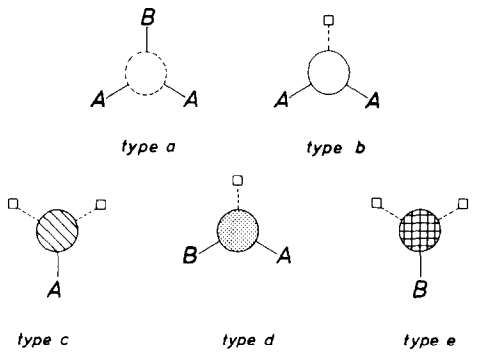

FIG. 6. Types of oxygen anions in the scheelite structure (see Fig. 5). A = eight-coordinated cation site (bismuth or iron); B = tetrahedral cation site (vanadium, molybdenum, or iron); □ = missing coordination of A or B cation type.

two of type *b*, one of type *c* and one of type *d*. The removal of an A cation, such as occurs when a bismuth vacancy is present in the lattice, generates two oxygens of type *c* ($2b \rightarrow 2c$), one of type *e* ($d \rightarrow e$) and four of type *d* ($4a \rightarrow 4d$).

Again, on the (101) plane, as well as on the (111) or (001) planes, where surface oxygen anions of type *b*, *c*, *d*, and *e* exist, the removal of an A cation will produce five oxygens of type *d* ($5a \rightarrow 5d$), one of type *e* ($d \rightarrow e$), and one of type *c* ($b \rightarrow c$).

In conclusion the significant role of the A-type cation vacancies in the scheelite structure is confirmed (*2*). However, the presence of cation vacancies not only does not discount the bismuth role in allyl formation (*5, 10, 12*), but it enhances it by generating higher bond order of Bi–Ox centers (type *c*) or anionic centers of type *d*.

Another aspect to be considered is the surface dehydration process which causes elimination of water from surface hydroxyls. The water desorption will favor the formation of a surface anionic vacancy on the less positively charged position (A cation site), while an O^{2-} ion will be left on the more positively charged position (B cation site). Indeed, in view of its more basic character, it is reasonable to assume that $(OH)^-$ is preferentially cleaved from Bi^{3+} rather than from Mo^{6+}. In summary, it results that A cations will be coordinatively more unsaturated with respect to B cations, and could be good sites for adsorption of olefin. These considerations (presence of A cation site vacancy and dehydration process) point to a predominant role of A cations in the first olefin activation step.

The experimental evidence shows a significant difference in catalytic behavior between the series of solid solutions with *Me* = Bi, where the bismuth content increases with *y*, and that with *Me* = Fe, where bismuth remains constant with *y*. These differences, fundamentally related to the solid state structure and chemistry of the catalyst, clearly point to a remarkable role of eight-coordinated cations in allyl formation: these ions are Bi sites until cation vacancies are present (Fig. 2), and Fe sites if there are no vacancies remaining (Fig. 3). Hence, eight-coordinated iron can account for the difference (especially in the absence of vacancies) in catalytic behavior between the two series of catalysts.

The eight-coordinated iron may even affect the α-hydrogen abstraction step favoring electron transfer from the olefin to the catalyst which is clearly associated with the reduction process of the solid. An ESCA study performed *in situ* and concerning the redox process of the catalyst components (Bi, Mo, V, and Fe) is in progress in our laboratory to support this hypothesis and to examine directly the reducibility of the different catalysts.

Moreover, some of the samples have been analyzed by thermogravimetry, reflectance spectroscopy, magnetic susceptibility, and X-ray diffraction in order to study their reduction in a H_2 atmosphere in the temperature range up to 600°C. The results have shown that the iron-containing catalysts are more easily reducible than the iron-free compounds (*21*).

A good reducibility is indeed known (*22*) to be essential for activity and selectivity of bismuth–molybdenum-based catalysts. In fact among several Bi–Mo catalysts studied

(*22*) the rate of catalyst reduction was higher for the multicomponent system used commercially.

Thus the presence of iron (*3, 23, 24*) in our catalysts clearly enhances the efficiency of the redox cycle; in fact, the redox couple Fe^{3+}/Fe^{2+}, operating in a scheelite matrix containing the essential elements bismuth and molybdenum as well as cation vacancies of eight-coordinated A type, decreases the energy of the pathway (Table 1) for catalytic event, by prompting electron and oxygen transfer between the bulk and the surface.

ACKNOWLEDGMENT

The authors would like to thank Mr. M. Inversi for the drawings.

REFERENCES

1. Grasselli, R. K., and Burrington, J. D., "Advances in Catalysis," Vol. 30, p. 133. Academic Press, New York, 1981.
2. Sleight, A. W., *in* "Advanced Materials in Catalysis" (J. J. Burton and R. L. Garten, Eds.), p. 181–208. Academic Press, New York, 1977.
3. Keulks, G. W., Krenzke, L. D., and Notermann, T. N., "Advances in Catalysis," Vol. 27, p. 183. Academic Press, New York, 1978.
4. Bielanski, A., and Haber, J., *Catal. Rev. Sci. Eng.* **19,** 1 (1979).
5. Grasselli, R. K., Burrington, J. D., and Brazdil, J. F., *Faraday Discuss. Chem. Soc.* **72,** 203 (1982).
6. Gates, B. C., Katzer, J. R., and Schuit, G. C. A., *in* "Chemistry of Catalytic Processes," p. 352. McGraw–Hill, New York, 1979.
7. Matsuura, I., *J. Catal.* **33,** 420 (1974); **35,** 452 (1974).
8. Matsuura, I., and Schuit, G. C. A., *J. Catal.* **25,** 314 (1972).
9. Haber, J., and Grzybowska, B., *J. Catal.* **28,** 489 (1973).
10. Grzybowska, B., Haber, J., and Janas, J., *J. Catal.* **49,** 150 (1977).
11. Linn, W. J., and Sleight, A. W., *J. Catal.* **41,** 134 (1976).
12. Brazdil, J. F., Glaeser, L. C., and Grasselli, R. K., *J. Catal.* **81,** 142 (1983).
13. Anichini, A., De Rossi, S., Gazzoli, D., Lo Jacono, M., Minelli, G., Porta, P., and Valigi, M., Ital. Patent 49573A81 (1981).
14. Porta, P., Lo Jacono, M., Valigi, M., Minelli, G., Anichini, A., De Rossi, S., and Gazzoli, D., *J. Catal.* **100,** 86–94 (1986).
15. Adams, C. R., Voge, H. H., Morgan, C. Z., and Armstrong, W. E., *J. Catal.* **3,** 379 (1964).
16. Callahan, J. L., Grasselli, R. K., Milberger, E. C., and Strecker, M. A., *Ind. Eng. Chem. Prod. Res. Dev.* **6,** 134 (1970).
17. Bassett, D. W., and Habgood, H. W., *J. Phys. Chem.* **64,** 769 (1960).
18. Adams, C. R., and Jennings, T. J., *J. Catal.* **3,** 549 (1964).
19. Sachtler, W. M. H., and De Boer, N. K., *in* "Proceedings, 3rd International Congress on Catalysis, Amsterdam, 1964," Vol. 1, p. 252. North-Holland, Amsterdam, 1965.
20. Burrington, J. D., Kartisek, C. T., and Grasselli, R. K., *J. Catal.* **63,** 235 (1980).
21. Valigi, M., De Rossi, S., Gazzoli, D., and Porta, P., *Gazz. Chim. Ital.* **116,** 97 (1986).
22. Brazdil, J. F., Suresh, D. D., and Grasselli, R. K., *J. Catal.* **66,** 347 (1980).
23. Wolfs, M. W. J., and Batist, Ph. A., *J. Catal.* **32,** 25 (1974).
24. Wolfs, M. W. J., and van Hooff, J. H. C., *in* "Preparation of Catalysts" (B. Delmon, P. A. Jacobs, and G. Poncelet, Eds.), p. 161. Elsevier, Amsterdam, 1976.